Planktic foraminifera shell chemistry response to seawater chemistry: Pliocene-Pleistocene seawater Mg/Ca, temperature and sea level change

David Evans[1†*], Chris Brierley[2], Maureen E. Raymo[3], Jonathan Erez[4] & Wolfgang Müller[1]

[1] *Department of Earth Sciences, Royal Holloway University of London, UK*

[2] *Department of Geography, University College London, UK*

[3] *Lamont-Doherty Earth Observatory, Columbia University, USA*

[4] *Earth Science Institute, The Hebrew University of Jerusalem, Israel*

[†] *Now at: Department of Geology and Geophysics, Yale University, New Haven, CT 06511, USA*

[*] *d.evans@yale.edu*

ABSTRACT

Foraminifera Mg/Ca paleothermometry forms the basis of a substantial portion of ocean temperature reconstruction over the last 5 Ma. Furthermore, coupled Mg/Ca-oxygen isotope ($\delta^{18}O$) measurements of benthic foraminifera can constrain eustatic sea level (ESL) independent of paleo-shoreline derived approaches. However, this technique suffers from uncertainty regarding the secular variation of the Mg/Ca seawater ratio (Mg/Ca_{sw}) on timescales of millions of years. Here we present coupled seawater-test Mg/Ca-temperature laboratory calibrations of *Globigerinoides ruber* in order to test the widely held assumptions that (1) seawater-test Mg/Ca co-vary linearly, and (2) the Mg/Ca-temperature sensitivity remains constant with changing Mg/Ca_{sw}. We find a nonlinear Mg/Ca_{test}-Mg/Ca_{sw} relationship and a substantial lowering of the Mg/Ca-temperature sensitivity at lower than modern Mg/Ca_{sw} from 9.0%°C^{-1} at Mg/Ca_{sw} = 5.2 mol mol^{-1} to 7.5±0.9%°C^{-1} at 3.4 mol mol^{-1}. Using our calibrations to more accurately calculate the offset between Mg/Ca and biomarker-derived paleotemperatures for four sites, we derive a Pliocene Mg/Ca_{sw} ratio of ~4.3 mol mol^{-1}. This

25 Mg/Ca_{sw} implies Pliocene ocean temperature 0.9-1.9°C higher than previously reported and, by
26 extension, ESL ~30 m lower compared to when one assumes that Pliocene Mg/Ca_{sw} is the same as at
27 present. Correcting existing benthic foraminifera datasets for Mg/Ca_{sw} indicates that deep water
28 source composition must have changed through time, therefore seawater oxygen isotope
29 reconstructions relative to present day cannot be used to directly reconstruct Pliocene ESL.
30
31 **1 INTRODUCTION**
32 The temperature-dependant incorporation of Mg/Ca into the calcite test of marine organisms,
33 principally foraminifera, is widely used to reconstruct the thermal evolution of the oceans
34 throughout the Cenozoic [e.g. Wara et al. 2005; Lear 2000]. Coupled Mg/Ca-oxygen isotope ($\delta^{18}O$)
35 measurements of the same or coeval foraminifera enable the $\delta^{18}O$ palaeotemperature equation to
36 be solved for $\delta^{18}O_{sw}$, with particular utility to benthic species, as the isotopic composition of the
37 deep ocean is less spatially variable. A consequence of this is that temporal trends in deep ocean
38 $\delta^{18}O_{sw}$ may be related to global ice volume [e.g. Lear et al. 2000], and by extension, sea level
39 [Sosdian & Rosenthal 2009; Woodard et al. 2014; Dwyer & Chandler 2009]. Much effort in this
40 direction has focused on unravelling the Pliocene-Pleistocene evolution of the major ice sheets and
41 the temperature of the oceans. In particular, there is considerable community interest in the
42 Pliocene Warm Period (3.264-3.205 Ma), as it is thought to represent the most recent period of
43 geological time with an atmospheric CO_2 concentration greater than preindustrial [Seki et al. 2010].
44 A confounding factor for Mg/Ca palaeothermometry is that the incorporation of most trace
45 elements into the shells of foraminifera is dependent on their respective concentration in seawater
46 [e.g. Delaney et al. 1985; Evans et al. 2015]. Whilst many studies have attempted to correct for this,
47 virtually all previous work assumes that shell Mg/Ca (Mg/Ca_{test}) varies linearly with seawater Mg/Ca
48 (Mg/Ca_{sw}). However, for all species studied to date – and inorganic precipitates – this has been
49 shown to be incorrect [Mucci & Morse 1983; Segev & Erez 2006; Evans et al. 2015]. Furthermore,
50 whilst much recent work has been focused on reconstructing Cenozoic Mg/Ca_{sw} [Fantle & DePaolo

2006; Coggon et al. 2010; Evans et al. 2013; Horita et al. 2002], the application of an appropriate correction for this secular variability to foraminifera data is confounded by the lack of accurate and temporally continuous Mg/Ca_{sw} reconstructions for all geological periods. Because both Mg and Ca have relatively long residence times in the ocean (~14 and ~1 Ma respectively [Li 1982]), most studies applying this proxy to Pliocene-Pleistocene samples assume that Mg/Ca_{sw} has remained constant over this time [e.g. Wara et al. 2005], although with at least one exception [Medina-Elizalde et al. 2008]. However, multiple lines of evidence suggest that this may not be the case [Horita et al. 2002; Fantle & DePaolo 2006]. These studies suggest a rise in Mg/Ca_{sw} from 3-4 mol mol^{-1} in the mid/late Pliocene to 5.2 mol mol^{-1} at present, with the direct implication that uncorrected Mg/Ca data would underestimate Pliocene warmth. Recently, O'Brien et al. [2014] found an offset between Mg/Ca and TEX_{86}^{H} temperature reconstructions during the Pliocene for ODP Site 1143 (South China Sea), which they argued is most likely caused by secular change in Mg/Ca_{sw}.

In the tropics, Pliocene Warm Period (PWP) Mg/Ca-derived sea surface temperature (SST) reconstructions suggests the West Pacific Warm Pool was 2-3°C warmer after accounting for this secular Mg/Ca_{sw} change [O'Brien et al. 2014] with a reduced or absent equatorial Pacific temperature gradient [Wara et al. 2005; Fedorov et al. 2013; Zhang et al. 2014]. These observations are only in partial agreement with climate models, which do not exhibit a similar magnitude of change in these gradients [Haywood et al. 2013; Brierley 2015]. Potential mechanisms of reconciling this proxy-model discrepancy include enhanced tropical cyclones [Fedorov et al. 2010] and altered cloud radiative properties [Burls & Fedorov 2014]. Accurate knowledge of SST and temperature gradients is required to assess which mechanism, if any, is the most appropriate.

This study presents the first detailed calibrations between Mg/Ca_{test}-Mg/Ca_{sw} for the planktic foraminifera *Globigerinoides ruber* (white, *sensu stricto*). Crucially, we also present a Mg/Ca_{test}-temperature calibration at below-modern Mg/Ca_{sw} (3.4 mol mol^{-1}), which enables us to test the widely-held assumption that the sensitivity of this thermometer does not change with

77 Mg/Ca_{sw}. Although these calibrations provide a basis for more accurate palaeothermometry
78 throughout the Cenozoic, here we focus on the implications of these data for the Pliocene-
79 Pleistocene for two reasons: firstly, there are published *G. ruber* records, which means that
80 uncertainties regarding the applicability of our calibrations to other or non-extant species can be
81 eliminated. Secondly, based on such records, we are able to reconstruct secular Mg/Ca_{sw} variability
82 over this time using the Mg/Ca-biomarker temperature offset technique of O'Brien et al. [2014].
83 This approach assumes that the differential temperature reconstructed by the two proxies is the
84 result of a lower than present-day Mg/Ca_{sw} ratio, resulting in a bias of Mg/Ca-derived temperatures
85 to lower values. However, the results of O'Brien *et al*. [2014] require revision because the
86 relationship between Mg/Ca_{test}-Mg/Ca_{sw}-temperature was not previously known in detail.
87 Furthermore, geochemical records may be biased by other factors, such as a shift in the seasonality
88 of a given proxy or the intensity of carbonate dissolution through time. This is indicated by the
89 differential magnitude of biomarker and Mg/Ca SST discrepancies between the East and West
90 Pacific [Dekens et al. 2008]. Therefore, the Mg/Ca_{sw} record of O'Brien et al. [2014], based on data
91 from one site, may be biased. We address this issue by utilising coupled Mg/Ca-biomarker proxy
92 data at four sites spanning the last ~5 Ma from which both proxies are available. Based on our new
93 Mg/Ca_{sw} record for this time interval, we then assess the implications of our results for coupled
94 Mg/Ca-$\delta^{18}O$-derived ice volume and eustatic sea level (ESL) estimates for the Pliocene.
95
96 **2 METHODS**
97 **2.1 *G. ruber* Mg/Ca_{test}-Mg/Ca_{sw}-temperature calibration**
98 **2.1.1 Experimental setup**
99 Foraminifera were collected from the northernmost Red Sea (Gulf of Eilat) at 20 m water depth by
100 plankton drift tows at a location with a bathymetry of >300 m. Foraminifera were immediately
101 picked from plankton concentrates to recovery dishes, whereupon they were measured,
102 photographed and transferred to individual 120 ml culture jars if they accepted a juvenile *Artemia*

103 brine shrimp, and fed daily. Individual foraminifera were cultured until they underwent
104 gametogenesis (usually < 7 days [see also Kisakürek et al. 2008]), and were transferred to new jars if
105 algal growth was detected.
106 All culture seawater was isotopically labelled to facilitate unambiguous identification of
107 chambers precipitated exclusively in culture. ^{135}Ba was chosen as the seawater spike because highly
108 enriched (93.5%) $^{135}BaCO_3$ is relatively inexpensive, and the low seawater [Ba] (<10 ppb) means little
109 spike (74 nM) is required to greatly modify the isotopic composition of large volumes of seawater.
110 Resulting culture seawater $^{135}Ba/^{138}Ba$ depended on the initial seawater [Ba] that in turn varied with
111 the proportion of Mg-free artificial seawater used to create seawater with variable Mg/Ca ratios
112 from artificial-natural seawater mixes; the artificial seawater used in this study was characterized by
113 [Ba] 2× that of Gulf of Eilat seawater. Culture seawater $^{135}Ba/^{138}Ba$ ratios varied between 0.52-1.82
114 (at Mg/Ca_{sw} = 2.2 and 5.2 respectively), which are easily distinguishable from natural (0.09194) by
115 laser-ablation ICPMS.
116 Two principal calibrations were carried out: (1) Mg/Ca_{test}-Mg/Ca_{sw} between Mg/Ca_{sw} = 2.2-
117 6.2 mol mol^{-1} at 26°C and (2) Mg/Ca-temperature between 20-30°C at Mg/Ca_{sw} = 3.4 mol mol^{-1}. Each
118 calibration consisted of five data points with 10-20 individual specimens cultured at each unique set
119 of conditions. The Mg/Ca ratio of seawater was modified by mixing natural Gulf of Eilat seawater
120 with artificial Mg-free seawater (i.e seawater [Ca] was constant), salinity was 37‰ in all
121 experiments.
122 **2.1.2 Laser-ablation ICPMS analysis**
123 Specimens were ultrasonicated in ~10% NaOCl and rinsed in deionized water, mounted on carbon
124 tape and analysed for X/Ca ratios using the 193 nm ArF laser-ablation ICPMS setup with two-volume
125 cell at Royal Holloway University of London [Müller et al. 2009]. The analytical procedures for
126 foraminifera, as well as a detailed description of carbonate trace element data quality are described
127 in the main text and supporting material of Evans et al. [2015]. Mg/Ca accuracy±precision (2SD) is
128 2±4% based on analysis of the standards NIST610 and MPI-DING GOR128. Briefly, we utilise slow

depth profiling in order to maximise vertical spatial resolution through the chamber walls. Ablation parameters were: 44-57 µm spot size, 2 Hz laser repetition rate. A 'squid' inline signal smoothing device was used to eliminate spectral skew at low repetition rates. Ba isotope data quality was optimised by increasing the m/z = 135 dwell time to 100 ms (~1/3 total dwell time), the maximum practically possible given the simultaneous requirements to monitor 10 other m/z and to keep the total ICPMS sweep time below 0.35 s. Whilst unnecessary for samples grown in cultured seawater with $^{135}Ba/^{138}Ba$ >0.5, the relatively low natural abundance of ^{135}Ba means that this is necessary to obtain suitably precise $^{135}Ba/^{138}Ba$ ratios, given the low (1-2 ppm) Ba concentration in foraminiferal calcite.

The 2SD of *G. ruber* chambers that were never exposed to ^{135}Ba-spiked seawater (n = 23) is 26.5% (see the supplementary material for further details). Only chambers characterized by $^{135}Ba/^{138}Ba$ within error of the culture seawater were used to define calibration equations. An example of this is shown in figure 1 using experiment DE3-2-26 (Mg/Ca_{sw} = 2.2 mol mol^{-1}, temperature = 26°C). Because these foraminifera grew in culture seawater with Mg/Ca ~40% of natural, chambers with elevated $^{135}Ba/^{138}Ba$ are characterised by lower Mg/Ca_{test} ratios than those with natural $^{135}Ba/^{138}Ba$ (or a mixture of the two). In order to avoid potential bias by integrating data from partial chamber wall profiles with variable $^{135}Ba/^{138}Ba$, only chambers with consistently elevated Ba-isotope ratios were used to define the calibrations. Some chambers are characterized by intermediate $^{135}Ba/^{138}Ba$ ratios because these foraminifera add a layer of calcite to the existing shell when a new chamber is formed. Mean values were integrated from the entire chamber wall in order that our laser-ablation measurements are directly comparable to solution analysis of dissolved tests. Unlike calibrations based on bulk (solution) analysis of multiple individuals, this method eliminates the need for mass-balance corrections for material precipitated prior to culture, which adds uncertainty if the proportion of calcite precipitated prior to collection is poorly constrained. Given the ease with which seawater $^{135}Ba/^{138}Ba$ can be modified, ^{135}Ba isotope spikes are an effective method of unambiguously identifying foraminifera calcite precipitated in culture,

155 **2.1.3 Seawater ICPMS analysis**

156 Trace element data quality as measured by ICPMS at the NERC Isotope Geosciences Laboratory
157 (British Geological Survey, UK) is described in Evans et al. [2015]. The procedure was not modified
158 except to include ^{135}Ba. Measured ^{135}Ba/^{138}Ba was normalised to a BGS QC seawater with natural
159 ^{135}Ba/^{138}Ba ([Ba] = ~300 ppm). The magnitude of this accuracy correction is 2.8%, following which
160 data quality (accuracy±precision) based on triplicate analysis of the seawater standard NASS-4 ([Ba]
161 = ~7 ppm) was 2.0±3.9% (2SD).

162 **2.2 Dataset treatment**

163 In order to examine secular variation in Mg/Ca_{sw} over the last 5 Ma, we utilise published
164 Mg/Ca and TEX_{86} data from ODP Site 806 [Wara et al. 2005; Zhang et al. 2014], Mg/Ca and $U^{K'}_{37}$ data
165 from ODP Site 847 [Dekens et al. 2007; Wara et al. 2005], Mg/Ca, $U^{K'}_{37}$ and TEX_{86} data from ODP
166 Site 1143 [Li et al. 2011; Tian et al. 2006; O'Brien et al. 2014; Zhang et al. 2014] and Mg/Ca and $U^{K'}_{37}$
167 data from ODP Site 999 [Seki et al. 2010; Schmidt et al. 2006; Badger et al. 2013; O'Brien et al.
168 2014], see figure 2. Only $U^{K'}_{37}$ data below saturation was used; therefore no temperature record
169 before 3.6 Ma is available from Site 999 and only TEX_{86} data was used at Site 1143 prior to 2.7 Ma.
170 Following dissolution and species-offset corrections (see below), Mg/Ca and biomarker datasets for
171 each site were LOWESS-smoothed and re-sampled at 100 ka resolution with the exception of Site
172 999 (250 ka). These data were then used to iteratively back-calculate Mg/Ca_{sw} for each site based on
173 our coupled Mg/Ca_{sw}-Mg/Ca_{test}-temperature calibration (see below), using the smoothed biomarker
174 temperatures from each site to solve for Mg/Ca_{sw}. Finally, calculated Mg/Ca_{sw} values from each site
175 were combined and LOWESS-smoothed to produce an average Mg/Ca_{sw} curve for the last 5 Ma.

176 Because our calibrations are based on *G. ruber*, yet much of the published SST data are
177 derived from *G. sacculifer*, fossil *G. sacculifer* Mg/Ca data were adjusted to *G. ruber* before
178 calculating Mg/Ca_{sw}. We do this based on the difference in the pre-exponential coefficient between
179 published laboratory Mg/Ca-temperature calibrations of the two species in modern seawater
180 [Nürnberg et al. 1996; Kisakürek et al. 2008], because unlike sediment trap or core top calibrations,

these analyses are less likely to be biased by dissolution or diagenesis. In line with previous studies [e.g. Anand et al. 2003], we use an exponential coefficient of 0.09 for both species in modern seawater. Based on this assumption, *G. ruber* and *G. sacculifer* have pre-exponential constants of 0.43 and 0.39 respectively, which equates to a temperature-independent offset of 10.3%. A high-resolution record for both species exists for Site 999 (Caribbean Sea) between ~3.4-2.2 Ma, enabling an assessment of the accuracy of this correction through time, and for foraminifera growing in seawater with potentially variable Mg/Ca (figure SM5). Because our correction is defined by foraminifera growing in modern seawater, it is useful to confirm that it also reliably adjusts a fossil record, when conditions were different to modern. LOWESS-smoothed curves of this portion of the dataset show high coherence. Because our Mg/Ca_{sw} record indicates that this ratio was lower than present over this time interval (section 3.2), this demonstrates that a correction applied in this way is not biased in the past by variable Mg/Ca_{sw}. Therefore, our *G. ruber*-derived calibrations can be applied with confidence to *G. sacculifer* data.

A dissolution correction is necessary to counter the effects of the preferential loss of relatively high-Mg portions of the foraminifera test when exposed to seawater with $\Delta[CO_3^{2-}]$ <~21 µmol kg^{-1} [see Dekens et al. 2002; Regenberg et al. 2014; Fehrenbacher & Martin 2014]. We considered two options for dissolution correction of the Mg/Ca data. Most previous work [e.g. Wara et al. 2005; O'Brien et al. 2014] utilises location-specific Mg/Ca-temperature calibrations with a depth correction applied to the exponential constant, such as those of Dekens et al. [2002]. However, we derive an alternative approach based on the assumption that Mg/Ca and biomarker-derived palaeotemperature reconstructions should be the same over the last four glacial-interglacial cycles. All of these proxies are frequently related to the same environmental variable (SST), and Mg/Ca_{sw} can be assumed to be invariant over this time. In order to apply this correction to all sites, the Mg/Ca and biomarker temperatures are matched over the past 400 ka by applying a constant multiplicative offset to the Mg/Ca data. This method implicitly assumes that the offset between proxies over this time is the combined result of seasonal differences in the proxies and

207 Mg/Ca dissolution. The latter of these effects is likely to be more important given the minimal
208 seasonality at most of the sites included in this study. There are two advantages of this approach:
209 (1) it requires no assumption regarding the relationship between core depth or core site carbonate
210 chemistry and dissolution, as opposed to previously suggested dissolution corrections [e.g. Dekens
211 et al. 2002], which may be inaccurate outside of the region in which they were defined. (2) It
212 eliminates potential problems regarding the application of culture calibrations to fossil data, as the
213 dissolution correction forces the Mg/Ca data to match the biomarkers. Nonetheless, a comparison
214 of both approaches is given in the supporting material, demonstrating that the correction method
215 exerts a small control on our results.
216
217 **3 RESULTS: Mg/Ca_{test} response to variable Mg/Ca_{sw} and temperature**
218 Trace element chemistry, $^{135}Ba/^{138}Ba$ ratios, carbonate chemistry details and culture
219 conditions for all experiments are given in table 1. Our calibrations are shown in figure 3 in
220 comparison to a previous *G. ruber* Mg/Ca-temperature calibration at modern day Mg/Ca_{sw} (5.2 mol
221 mol^{-1}) carried out in the same laboratory [Kisakürek et al. 2008], see figure 3B. The Mg/Ca_{sw}-
222 Mg/Ca_{test} calibration (figure 3A) confirms the nonlinear response to Mg/Ca_{sw} observed in other
223 foraminifera [Segev & Erez 2006; Evans et al. 2015]:
224 $$Mg/Ca_{test} = -0.0591 \pm 0.0264 \times Mg/Ca_{sw}^{2} + 1.15 \pm 0.14 \times Mg/Ca_{sw} \quad (1)$$
225 $R^2 = 0.99$, n = 76, 95% confidence intervals. Although previous studies have argued that a power
226 regression most appropriately describes the variation of Mg/Ca_{test} with Mg/Ca_{sw} [Ries 2004; Evans &
227 Müller 2012], we present this relationship as a quadratic regression forced through the origin,
228 because the linear D_{Mg}-Mg/Ca_{sw} relationship (figure SM3) implies this [see also Evans et al. 2015].
229 This does not affect the conclusions of Evans & Müller [2012], as the shape of this relationship is
230 similar to a power curve (with $0<H<1$, where H is the power component of a seawater-shell Mg/Ca
231 calibration of the form: $Mg/Ca_{test} = F \times Mg/Ca_{sw}^{H}$), in that it is offset to higher Mg/Ca_{test} at a given
232 Mg/Ca_{sw} compared to a linear regression over the range 0-5.2 mol mol^{-1}.

The Mg/Ca-temperature relationship at Mg/Ca_{sw} = 3.4 mol mol^{-1} (figure 3B) is described by the exponential curve:

$$Mg/Ca_{test} = 0.48 \pm 0.11 \times exp^{0.075 \pm 0.009T} \quad (2)$$

R^2 = 0.99, n = 44, 95% confidence intervals. Equation 2 defines a Mg/Ca-temperature sensitivity of 7.5%°C^{-1}. This is a significant reduction compared to calibrations in modern seawater for this species, where the exponential coefficient is routinely taken to be 0.09 [e.g. Anand et al. 2003], i.e. 9%°C^{-1}. Thus, the sensitivity of this thermometer is not constant at below-modern Mg/Ca_{sw} ratios.

Defining the surface that describes how Mg/Ca_{test}, Mg/Ca_{sw} and temperature co-vary in three dimensions (figure 3C) requires some assumption about the form that this relationship should take. Traditionally it has been assumed that the sensitivity of the Mg/Ca-temperature relationship does not change with Mg/Ca_{sw}. However, our calibrations demonstrate that this is not the case (equation 2), and we thus discount the possibility that only the pre-exponential constant of a Mg/Ca-temperature calibration varies with Mg/Ca_{sw}. Given this constraint, the coupled calibration surface shown in figure 3C was produced by assuming that the shape of the Mg/Ca-temperature relationship is always of the form $Mg/Ca = Bexp^{AT}$, where the two coefficients vary as a function of Mg/Ca_{sw}.

Five different assumptions were made regarding the relationship between these coefficients and Mg/Ca_{sw}: invariant, linear, power, exponential or quadratic, producing a total of 20 different equations. These surfaces were then least-squares modeled to fit the *G. ruber* laboratory culture-derived calibration lines. Figure 4 shows the results of this exercise, including modelled variation in the coefficients of a Mg/Ca-temperature calibration with changing Mg/Ca_{sw} (figure 4C,D). Red lines are models that deviate from the data by less than 0.1 mmol mol^{-1} on average, whilst grey lines are those that are offset by more than this, and therefore do not accurately match the calibrated relationships. We find that the model surface best matches all the observed features of the data (e.g. convex upwards Mg/Ca_{test}-Mg/Ca_{sw} relationship as well as the reduced Mg/Ca-temperature sensitivity at lower Mg/Ca_{sw}) when both coefficients vary quadratically with Mg/Ca_{sw},

(see the supporting material for further details). Specifically, if the pre-exponential constant is held constant, the models generally produce convex-downwards Mg/Ca_{test}-Mg/Ca_{sw} relationships, which is the opposite of what we observe (figure 4A; Evans et al. [2015]). Although several of the models deviate from the data by less than 0.1 mmol mol^{-1} on average (some other models cannot be statistically excluded), only one accurately fits all three empirical calibrations, as well maintaining the observed Mg/Ca-temperature sensitivity decrease and the minimal variation in the pre-exponential coefficient that we observe (figure 4C). The equation of the coupled calibration surface (figure 3C) is therefore modeled with the general form $Mg/Ca_{test} = B\exp^{AT}$, where:

$$B = 0.019 \times Mg/Ca_{sw}^{2} - 0.16 \times Mg/Ca_{sw} + 0.804 \quad (3)$$

And:

$$A = -0.0029 \times Mg/Ca_{sw}^{2} + 0.032 \times Mg/Ca_{sw} \quad (4)$$

Because a limited number of these models are capable of representing the calibration data, variation in the sensitivity of the Mg-temperature relationship (figure 4C) may be constrained by a small number of Mg/Ca-temperature calibrations at different Mg/Ca_{sw}, provided Mg/Ca_{test}-Mg/Ca_{sw} is also calibrated. This means that our coupled calibration should also be applicable to earlier Cenozoic reconstructions. Specifically, the variation in the Mg/Ca_{test}-temperature gradient at Mg/Ca_{sw} below 3.4 mol mol^{-1} is better constrained than it appears from figure 4D. This is because it is not possible to fit the variation in this coefficient with Mg/Ca_{sw} using most of the surface models that we tested, given the simultaneous requirement to match the modelled Mg/Ca_{test} variation with the Mg/Ca_{test}-Mg/Ca_{sw} calibration. Although more complex functions may be written that would allow better calibration-model matching with a constant pre-exponential coefficient, it is more parsimonious to assume some variation in both coefficients; our chosen 'double quadratic' model is the simplest way of producing a good model-data fit. It exactly matches the observed Mg/Ca-temperature sensitivity decrease at lower Mg/Ca_{sw}, and maintains the pre-exponential constant between 0.45-0.5 over the range Mg/Ca_{sw} = 2-6 mol mol^{-1}, as observed. However, it should not be used to extrapolate beyond this range, and the uncertainty in the sensitivity of this thermometer

below Mg/Ca_{sw} = 3 mol mol^{-1} (figure 4D) should be propagated into earlier Cenozoic relative temperature reconstructions.

4 DISCUSSION

4.1 Pliocene-Recent Mg/Ca_{sw} reconstruction

Foraminifera Mg/Ca data from all four sites are shown in figure 5A. At face value, these records imply that the Pliocene tropics were the same temperature or cooler than present, with the exception of Site 847. Mg/Ca-derived paleotemperatures are offset to values 5-15% lower compared to those derived from biomarkers from the same site during the Pliocene (figure 5B). Site-specific back-calculated Mg/Ca_{sw}, derived from these offsets and our calibration surface (figure 3C), is shown in figure 5C. Those derived from Site 1143 and 806 are in excellent agreement throughout the last 5 Ma, both in terms of the finer detail in these records as well as the absolute magnitude of Pliocene-Recent Mg/Ca_{sw} rise. Because we utilise both TEX_{86} and $U^{K'}_{37}$ data at Site 1143, this cannot be a result of a potential bias on the TEX_{86} data, e.g. subsurface cooling. The Site 999 record is broadly in good agreement with these, and the most likely explanation for the apparent offset between this and the other records between ~0.5-1.5 Ma is the poor temporal resolution of both the alkenone and Mg/Ca datasets at Site 999 between 0-2 Ma. In contrast to these three sites, the biomarker and Mg/Ca data from Site 847 show little proxy disagreement over the past 5 Ma [Dekens et al. 2008], and consequently the Mg/Ca_{sw} record calculated from these datasets is in poor agreement with that from other sites (figure 5C). However, the overall agreement between the Mg/Ca_{sw} records from the remaining three sites, in distinct basins, supports the hypothesis that the offset between the biomarker and Mg/Ca proxies over this interval is primarily the result of seawater chemistry change.

Figure 5D shows a Mg/Ca_{sw} reconstruction using data from all sites, in comparison to other proxy data. By averaging several records from different depths spanning a large portion of the tropics, our Mg/Ca_{sw} record minimizes temporally variable proxy complications at any one location. For this reason, we suggest that our reconstruction supersedes that of O'Brien et al. [2014].

311 Specifically, we present two back-calculated Mg/Ca_{sw} records, both with and without data from Site
312 847, the site that shows little biomarker-Mg/Ca temperature offset through the last 5 Ma. Two sets
313 of confidence bands (95%) are given with our Mg/Ca_{sw} record (figure 5D). These were produced
314 using 1000 bootstrap LOWESS fits through the data shown in figure 5C. The inner error is based
315 only on the variance between the sites, whilst the outer error applies a random ±2.5°C error to each
316 of the biomarker temperature records, in order to simulate potential seasonal or other bias between
317 the proxies through time. All data for our Mg/Ca_{sw} reconstructions including confidence bands is
318 given in the supporting material.

319 **4.2 Sources of error in biomarker-foraminifera Mg/Ca derived Mg/Ca_{sw}**

320 The deviation of the Mg/Ca_{sw} record based on Site 847 from those derived from other sites indicates
321 something fundamentally different about the relationship between Mg/Ca and biomarker-derived
322 SST at this location over the last 5 Ma compared to the other three locations. Consequently,
323 producing a back-calculated Mg/Ca_{sw} record that excludes data from Site 847 may be justified.
324 Although our preferred Mg/Ca_{sw} reconstruction does not exclude this dataset because it is difficult
325 to prove bias from other factors, it is this site which exhibits the highest present-day inter-annual
326 SST variability and it may therefore be the case that this Mg/Ca_{sw} reconstruction is affected by
327 changes in the seasonal and inter-annual bias of these proxies through time. In order to bring
328 reconstructed Mg/Ca_{sw} from Site 847 in line with the others during the Pliocene, *G. sacculifer*
329 production at this site would have to dominantly occur in seasons or years characterized by SST
330 ~2°C greater than the time of alkenone production, relative to today.

331 Aside from seasonality, the most significant source of inaccuracy may come from the
332 dissolution adjustment. For example, a higher Pliocene deep ocean $\Delta[CO_3^{2-}]$ compared to present
333 would result in reduced dissolution [Regenberg et al. 2014], and therefore Pliocene Mg/Ca-derived
334 temperatures would be overestimates as the dissolution correction would be too large. However,
335 the foraminifera shell weight data for Sites 806 and 847 [Wara et al. 2005] do not show any
336 significant difference in temporal trend between the East and West Pacific. Assuming shell weight

relates meaningfully to dissolution [see Rosenthal & Lohmann 2002], and would otherwise be relatively constant through time, this indicates that differential inter-site temporal variation in bottom water saturation state is unlikely to explain the offset in the Mg/Ca_{sw} reconstructions from these two sites. Because the SST used to calculate Mg/Ca_{sw} at Site 847 is entirely alkenone-derived, the proposed depth-integration effect of TEX_{86}, whereby a potentially shallower Pliocene thermocline biases this proxy to cooler temperatures [Seki et al. 2010], is also an unlikely explanation.

4.3 Mg/Ca_{sw} control on planktic Mg/Ca-paleothermometry

Our preferred record (figure 5D) including all sites, indicates that mean Pliocene and Pliocene Warm Period Mg/Ca_{sw} was 4.3 mol mol^{-1}. It follows from equation 4 that there was a minor reduction in the Mg/Ca-temperature sensitivity for *G. ruber* to 8.4%°C^{-1}. An increase in Mg/Ca_{sw} of 0.9 mol mol^{-1} since the Pliocene is consistent with our knowledge of the timescales of processes controlling the oceanic cycling of these elements. A change of this magnitude on a timescale of <5 Ma implies that oceanic [Ca] ($[Ca_{sw}]$) was 20% higher in the Pliocene, given the residence times of Mg and Ca (~14 and ~1 Ma respectively) [Li 1982]. Our record is in agreement with the fluid inclusion data of Horita et al. [2002], and implies a broadly similar magnitude of Mg/Ca_{sw} change over the last 3 Ma compared to the pore fluid modeling of Fantle & DePaolo [2006]. However, both this pore fluid model and the Mg/Ca_{sw} back-calculation of O'Brien et al. [2014] imply mid-Pliocene Mg/Ca_{sw} ~1-1.5 mol mol^{-1} lower than our reconstruction between 3-5 Ma (figure 5D). The reconstruction of O'Brien et al. [2014] is likely biased because it is based on one site, and the relationship between Mg/Ca_{test}-Mg/Ca_{sw}-temperature was not previously known in detail for any planktic foraminifera. The sub-Ma oscillations of the Mg/Ca_{sw} reconstruction of Fantle & DePaolo [2006] are largely controlled by the Ca isotope record utilised. Whilst our reconstruction falls within error of the $[Ca_{sw}]$ curve of that study, our data indicate Pliocene $[Ca_{sw}]$ was towards the upper limit of the range reported by those authors.

Based on our reconstruction, mid-late Pliocene planktic foraminiferal Mg/Ca-derived palaeotemperature underestimation (i.e. the difference between assuming no seawater chemistry change and using our Mg/Ca_{sw} record) ranges from ~1°C when Mg/Ca_{test} values are ~1 mmol mol^{-1} (SST = ~9°C) to ~1.8°C when Mg/Ca_{test} values are >5 mmol mol^{-1} (SST >30°C). Thus, tropical temperatures during the PWP are likely underestimated by 1.6-1.9°C. Because the magnitude of this correction is dependent on Mg/Ca_{test}, there is also an impact on estimated Pliocene SST gradients. This effect is relatively minor within the tropics, but may become important when comparing tropical to mid-latitude data (figure SM7).

Finally, our finding that the sensitivity of the Mg/Ca palaeothermometer varies with Mg/Ca_{sw} for planktic foraminifera has significant implications for studies reconstructing transient temperature variations in the Paleogene, when Mg/Ca_{sw} was ~50% of modern [e.g. Evans et al. 2013; Coggon et al. 2010]. For example, a mid-Eocene Mg/Ca_{sw} ratio of 2.5 mol mol^{-1} would imply a reduction in the exponential coefficient to 0.062 (from equation 4). This implies that Mg/Ca-derived relative temperature shifts over transient warming events in deep-time, such as the Paleocene-Eocene Thermal Maximum [e.g. Zachos et al. 2003], may be affected by this previously unconsidered source of error.

4.4 Mg/Ca_{sw} control on benthic Mg/Ca-paleothermometry

If Pliocene Mg/Ca_{sw} was lower as our reconstruction suggests, then foraminifera Mg/Ca-derived deep ocean temperatures have also been underestimated. The implications of this for bottom water palaeothermometry are difficult to assess because deep benthic foraminifera are difficult to culture and consequently the relationship between Mg/Ca_{test}-Mg/Ca_{sw} is poorly known. Evans & Müller [2012] describe in detail how the degree of non-linearity of this relationship may be indirectly calculated for *Oridorsalis umbonatus*, based on coupled Mg/Ca-$\delta^{18}O$ measurements of mid-Eocene specimens. This calculation is updated here to reflect new information regarding Eocene Mg/Ca_{sw} [Evans et al. 2013], and without the 'CCD-correction' suggested by Cramer et al. [2011]. Although quadratic functions best describe the Mg/Ca_{sw}-Mg/Ca_{test} relationship of at least

388 some foraminifera (section 3.1), we assume a power relationship of the form $Mg/Ca_{test} = F \times Mg/Ca_{sw}^{H}$
389 most appropriately describes the changing incorporation of Mg with seawater chemistry in benthic
390 foraminifera and derive H = 0.51 for *O. umbonatus*. Whilst direct corroboration of the form that this
391 relationship should take is lacking for these foraminifera, defining it in this way is advantageous in
392 that it retains consistency with previous work [Evans & Müller 2012; Woodard et al. 2014].
393 Moreover, the form of this regression is a relatively small source of error in the calculation. Whilst it
394 is possible that different benthic foraminifera are characterised by variable Mg/Ca_{test}-Mg/Ca_{sw}
395 relationships (see below), we initially explore the implication of secular Mg/Ca_{sw} on bottom water
396 palaeothermometry assuming this is not the case.
397 Figure 6 shows the extent to which benthic foraminifera Mg/Ca-derived temperature may
398 have been underestimated, based on our Mg/Ca_{sw} record (figure 5) and a calculated relationship
399 between seawater-test Mg/Ca for benthic foraminifera as described above. Applied to the
400 *Cibicidoides wuellerstorfi* data from DSDP Site 607 [Sosdian & Rosenthal 2009] and the *Uvigerina*-
401 derived record from ODP1208 [Woodard et al. 2014], this Mg/Ca_{sw} correction implies deep ocean
402 temperature has been underestimated by 0.9-1.4°C during the PWP, giving a mean North Atlantic
403 PWP bottom water temperature of 5.8°C. This correction places the North Atlantic benthic
404 foraminifera Mg/Ca record in good agreement with the PRISM dataset, which indicates that surface
405 ocean temperatures in the source region of North Atlantic Deep Water (NADW) were 4-5°C greater
406 than at present [Dowsett et al. 2009a; Dowsett et al. 2009b]. Conversely, using the PRISM dataset
407 to independently constrain H for *Cibicidoides*, by varying H until the Site 607 Mg/Ca record matches
408 these PRISM SST data (±1°C) gives H = 0.17-0.73 with a midpoint of 0.46. Although calculating H in
409 this way is associated with a large temperature-derived uncertainty, this result is in good agreement
410 with that derived for *O. umbonatus* using a completely different (Eocene) dataset. The likely
411 similarity of H between these two species has been previously noted [Cramer et al. 2011].
412 *Uvigerina* data are also available for Site 607 [Woodard et al. 2014], which means that a
413 value of H can also be calculated for this genus. We do this by minimizing the sum of squares of the

difference in temperature reconstructions for the two species, across the time interval that data for both species exist (see the supporting information for a detailed explanation). Constraining *Uvigerina* H in this way implicitly assumes that there is no non-thermal control other than Mg/Ca_{sw} that may differentially impact *Uvigerina* and *Cibicidoides*. Using this technique give H_{Uvi} = 0-0.46; the large uncertainty is the combined result of the uncertainty in H_{Cib} and because we allow for a 1°C potential offset between the temperatures recorded by the two species. These calculations suggest that *Uvigerina* may be relatively less sensitive to seawater chemistry change unless Mg/Ca_{sw} is substantially lower (<50%) than present. Whilst associated with large uncertainties, the salient point is that it is not safe to assume that all benthic foraminifera are characterized by identical seawater-test Mg/Ca relationships. The implications of these calculations are discussed in section 4.5 in relation to $\delta^{18}O_{sw}$ and ice volume.

4.5 Implications for Pliocene $\delta^{18}O_{sw}$ and sea level reconstruction

Given the Mg/Ca_{sw} control on Mg/Ca_{test} for three commonly utilised benthic foraminifera (section 4.4; [Evans & Müller 2012]), Pliocene deep ocean temperature, ice volume and $\delta^{18}O_{sw}$ reconstructions derived from such data, should be considered sensitive to Mg/Ca_{sw}. For example, the Atlantic-Pacific $\delta^{18}O_{sw}$ gradient prior to the onset of northern hemisphere glaciation at ~2.75 Ma reported by Woodard et al. [2014] is derived from two species, and is therefore highly sensitive to a difference in the value of H for *Uvigerina* and *Cibicidoides*. Figure 7 displays this sensitivity, in the context of the values of H that we reconstruct above. This graph shows the dependency of the reconstructed Site 1208-607 $\delta^{18}O_{sw}$ gradient on the value of H for the two species. For example, if *both* species were characterized by H = 0.3 (i.e. the relationship between seawater and shell Mg/Ca for this species is described by the equation $Mg/Ca_{test} = F \times Mg/Ca_{sw}^{0.3}$) then the reconstructed $\delta^{18}O_{sw}$ gradient would be -0.7. Based on the seawater-test Mg/Ca relationships derived in section 4.3, the inter-basin offset may fall anywhere between ~0.4-1.2‰. Whilst the originally reported gradient falls within this range, constraining this more precisely requires an improved assessment of seawater-test Mg/Ca relationships for these benthic foraminifera. This remains the case even if the

same species were to be used between sites, given that it has been argued that different temperature sensitivities should be applied to different sites [Woodard et al. 2014].

Revised benthic foraminifera-derived temperature and $\delta^{18}O_{sw}$ reconstructions are shown in figure 8 with error bands associated with the uncertainty in H for each species, in comparison to the records as they were originally published with no correction for secular variation in Mg/Ca_{sw}. Once corrected using our Mg/Ca_{sw} curve and species-specific estimation of H, the Mg/Ca data imply NADW 3-4°C warmer and Pacific Deep Water (PDW) broadly similar to present before 2.7 Ma. Ice volume and sea level estimates based on coupled benthic foraminifera Mg/Ca-$\delta^{18}O$ data are highly sensitive to a temperature revision of this magnitude. Using a $\delta^{18}O$-sea level relationship of 0.01‰ m^{-1} [Adkins et al. 2002] and the *Cibicidoides* $\delta^{18}O$-temperature calibration of Marchitto et al. [2014], a 1°C systematic bias in bottom water temperature translates to ~23.5 m error in inferred eustatic sea level (ESL). Therefore, a direct implication of our Mg/Ca_{sw} reconstruction is that assuming no seawater chemistry change since the Pliocene would result in an overestimation of ESL during the PWP. Furthermore, applying our correction to the data of Woodard et al. [2014] maintains a change in the Pacific-Atlantic inter-basin $\delta^{18}O_{sw}$ gradient between 2.8-2.6 Ma, which implies a shift in the source and/or isotopic composition of deep water through time. As a result, foraminifera and ostracod-based estimates of Pliocene sea level [Sosdian & Rosenthal 2009; Dwyer & Chandler 2009; Miller et al. 2012] should not be considered reliable when based purely on the difference between modern and palaeo-$\delta^{18}O_{sw}$ at a specific location.

Assuming no diagenetic or other source of temperature bias, the corrected Site 607 record implies reasonably consistent near-modern peak interglacial $\delta^{18}O_{sw}$, and by extension ice volume throughout the record (figure 8). This is in contrast to Site 1208, which shows peak PWP $\delta^{18}O_{sw}$ offsets >0.5‰ more negative than at present. This discrepancy is most easily explained by a reduced NADW component in PDW prior to the onset of northern hemisphere glaciation, as previously suggested [Woodard et al. 2014]. However, our Mg/Ca_{sw}-corrected reconstructions allow a more detailed explanation for the differential thermal and isotopic evolution of the two sites prior

466 to 2.7 Ma: Specifically: (1) NADW was evidently considerably warmer than at present (figure 8A),
467 consistent with North Atlantic SST at this time [Dowsett et al. 2009a]. (2) There was no NADW
468 component in PDW at Site 1208 before the onset of northern hemisphere glaciation. Given that the
469 corrected Site 607 record shows NADW 3-4°C higher than at present, which was not the case for
470 PDW and by extension Antarctic Bottom Water (AABW) (figure 8B), even a reduced NADW
471 component would result in PDW temperatures far higher than our corrected record indicates. (3)
472 Slightly fresher AABW (more negative $\delta^{18}O_{sw}$ by ~0.2-0.3‰) during the Pliocene is required in order
473 to reconcile the 0.5‰ peak $\delta^{18}O_{sw}$ offset from present, given that ESL was at most 20-30 m above
474 present-day [Woodard et al. 2014]. Finally, figure 8B shows that AABW obtained a modern
475 interglacial $\delta^{18}O_{sw}$ composition during the early stages of this transition, as by ~2.68 Ma peak
476 interglacial $\delta^{18}O_{sw}$ relative to modern (0 to -0.1‰) is in good agreement between the two sites. This
477 shift occurred concurrently with the relatively rapid rise in temperature at Site 1208 between 2.7-2.6
478 Ma and the introduction of a NADW component in PDW over this interval.
479
480 **CONCLUSION**
481 We present the first calibration of the response of planktic foraminifera Mg/Ca (*G. ruber*) to variation
482 in both temperature and Mg/Ca_{sw}, a prerequisite for any palaeoceanic study utilising foraminifera
483 Mg/Ca in sediments older than ~2 Ma. We use these calibrations to more accurately estimate
484 secular variation in Mg/Ca_{sw} over the last 5 Ma, assuming that the offset between Mg/Ca and
485 biomarker proxies from tropical sites for this time period is best explained by a shift in seawater
486 chemistry [e.g. O'Brien et al. 2014]. This approach assumes a constant temporal offset (which may
487 or may not be 0°C) between the water depth(s) that the Mg/Ca ratio of 'surface-dwelling' planktic
488 foraminifera and TEX_{86} represent. Because this may not be the case, our confidence intervals not
489 only account for inter-site variability but also include a possible relative shift of ±2.5°C between the
490 proxies. We find that Mg/Ca_{sw} during the Pliocene was 4.3 mol mol^{-1}, higher than previously
491 proposed [O'Brien et al. 2014] but 17% lower than at present. This implies both surface and deep

ocean Mg/Ca-derived temperatures have been underestimated by 0.9-1.9°C. Coupled Mg/Ca-$\delta^{18}O$-derived eustatic sea level reconstructions are sensitive to an inaccuracy of this magnitude. Correcting existing records using our Mg/Ca_{sw} reconstruction enables a clearer picture of Pliocene deep water formation and circulation to be established. We show that North Atlantic Deep Water was essentially absent in the Pacific before the onset of northern hemisphere glaciation, and that AABW was fresher (~-0.3‰) compared to present during the Pliocene Warm Period.

Finally, our *G. ruber* calibrations in 3D temperature-Mg/Ca_{test}-Mg/Ca_{sw} space enables us to tightly constrain how the sensitivity of the Mg/Ca thermometer changes with Mg/Ca_{sw}. This change is significant: the Mg/Ca increase per °C is reduced to ~8% for the Pliocene and ~6% for the Eocene, assuming that seawater [Mg] and [Ca] exert an equal control on this sensitivity. Thus, our findings also have important implications for the use of Mg/Ca for relative temperature reconstruction over climatic events throughout the Cenozoic, such as the Paleocene-Eocene hyperthermals and the Eocene-Oligocene Transition.

ACKNOWLEDGMENTS

DE acknowledges a NERC postgraduate studentship at RHUL. We are grateful to Shai Oron (Interuniversity Institute for Marine Sciences, Eilat) for help with plankton tows and to Tom Barlow and Simon Chenery (BGS, UK) for ICPMS trace element analysis of seawater samples. An Israeli Science Foundation Grant #551/10 to JE supported the foraminifera culturing work. MER acknowledges support from NSF grant OCE-12-02632. We are grateful to Yair Rosenthal and Michael Henehan for commenting on an earlier draft of this work. The constructive comments of Matthew Fantle and two anonymous reviewers greatly improved this contribution.

REFERENCES CITED

Adkins, J.F., McIntyre, K. & Schrag, D.P., 2002. The salinity, temperature, and delta18O of the glacial deep ocean. *Science (New York, N.Y.)*, 298(5599), pp.1769–73.

Anand, P., Elderfield, H. & Conte, M.H., 2003. Calibration of Mg/Ca thermometry in planktonic foraminifera from a sediment trap time series. *Paleoceanography*, 18(2).

518 Badger, M.P.S. et al., 2013. High-resolution alkenone palaeobarometry indicates relatively stable p
519 CO_2 during the Pliocene (3.3-2.8 Ma). *Philosophical transactions. Series A, Mathematical,*
520 *physical, and engineering sciences*, 371.

521 Brierley, C.M., 2015. Interannual climate variability seen in the Pliocene Model Intercomparison
522 Project. *Climate of the Past*, 11,pp.605-618.

523 Burls, N.J. & Fedorov, a. V., 2014. What Controls the Mean East–West Sea Surface Temperature
524 Gradient in the Equatorial Pacific: The Role of Cloud Albedo. *Journal of Climate*, 27(7), pp.2757–
525 2778.

526 Coggon, R.M. et al., 2010. Reconstructing past seawater Mg/Ca and Sr/Ca from mid-ocean ridge
527 flank calcium carbonate veins. *Science*, 327(5969), pp.1114–7.

528 Cramer, B.S. et al., 2011. Late Cretaceous–Neogene trends in deep ocean temperature and
529 continental ice volume: Reconciling records of benthic foraminiferal geochemistry ($\delta^{18}O$ and
530 Mg/Ca) with sea level history. *Journal of Geophysical Research*, 116, pp.1–23.

531 Dekens, P.S., Ravelo, A. C. & McCarthy, M.D., 2007. Warm upwelling regions in the Pliocene warm
532 period. *Paleoceanography*, 22, PA3211, doi: 10.1029/2006PA001394.

533 Dekens, P.S. et al., 2008. A 5 million year comparison of Mg/Ca and alkenone paleothermometers.
534 *Geochemistry, Geophysics, Geosystems*, 9(10).

535 Dekens, P.S. et al., 2002. Core top calibration of Mg/Ca in tropical foraminifera: Refining
536 paleotemperature estimation. *Geochemistry, Geophysics, Geosystems*, 3(4).

537 Delaney, M.L., Be, A.W.H. & Boyle, E.A., 1985. Li , Sr , Mg , and Na in foraminiferal calcite shells
538 from laboratory culture , sediment traps , and sediment cores. *Geochimica et Cosmochimica*
539 *Acta*, 49, pp.1327–1341.

540 Dowsett, H.J., Chandler, M. & Robinson, M.M., 2009a. Surface temperatures of the Mid-Pliocene
541 North Atlantic Ocean: implications for future climate. *Philosophical transactions. Series A,*
542 *Mathematical, physical, and engineering sciences*, 367, pp.69–84.

543 Dowsett, H.J., Robinson, M.M. & Foley, K.M., 2009b. Pliocene three-dimensional global ocean
544 temperature reconstruction. *Climate of the Past*, 5, pp.769–783.

545 Dwyer, G.S. & Chandler, M. a, 2009. Mid-Pliocene sea level and continental ice volume based on
546 coupled benthic Mg/Ca palaeotemperatures and oxygen isotopes. *Philosophical transactions.*
547 *Series A, Mathematical, physical, and engineering sciences*, 367(1886), pp.157–68.

548 Elderfield, H. et al., 2010. A record of bottom water temperature and seawater δ18O for the
549 Southern Ocean over the past 440kyr based on Mg/Ca of benthic foraminiferal Uvigerina spp.
550 *Quaternary Science Reviews*, 29(1-2), pp.160–169.

551 Evans, D. et al., 2013. Eocene seasonality and seawater alkaline earth reconstruction using shallow-
552 dwelling large benthic foraminifera. *Earth and Planetary Science Letters*, 381, pp.104–115.

553 Evans, D. et al., 2015. Mg/Ca-temperature and seawater-test chemistry relationships in the shallow-
554 dwelling large benthic foraminifera Operculina ammonoides. *Geochimica et Cosmochimica*
555 *Acta*, 148, pp.325–342.

556 Evans, D. & Müller, W., 2012. Deep time foraminifera Mg/Ca paleothermometry: Nonlinear
557 correction for secular change in seawater Mg/Ca. *Paleoceanography*, 27(4), p.PA4205.

558 Fantle, M. & DePaolo, D., 2006. Sr isotopes and pore fluid chemistry in carbonate sediment of the
559 Ontong Java Plateau: Calcite recrystallization rates and evidence for a rapid rise in seawater
560 Mg over the last 10 million years. *Geochimica et Cosmochimica Acta*, 70(15), pp.3883–3904.

561 Fedorov, a V et al., 2013. Patterns and mechanisms of early Pliocene warmth. *Nature*, 496(7443),
562 pp.43–9.

563 Fedorov, A. V, Brierley, C.M. & Emanuel, K., 2010. Tropical cyclones and permanent El Niño in the
564 early Pliocene epoch. *Nature*, 463(7284), pp.1066–70.

565 Fehrenbacher, J.S. & Martin, P.A., 2014. Exploring the dissolution effect on the intrashell Mg/Ca
566 variability of the planktic foraminifer Globigerinoides ruber. *Paleoceanography*, 29.

567 Haywood, A. M. et al., 2013. Large-scale features of Pliocene climate: results from the Pliocene
568 Model Intercomparison Project. *Climate of the Past*, 9(1), pp.191–209.

569 Horita, J., Zimmermann, H. & Holland, H.D., 2002. Chemical evolution of seawater during the
570 Phanerozoic : Implications from the record of marine evaporites. *Geochimica et Cosmochimica*
571 *Acta*, 66(21), pp.3733–3756.

572 Kisakürek, B. et al., 2008. Controls on shell Mg/Ca and Sr/Ca in cultured planktonic foraminiferan,
573 Globigerinoides ruber (white). *Earth and Planetary Science Letters*, 273(3-4), pp.260–269.

574 Lear, C.H., Elderfield, H. & Wilson, P.A., 2000. Cenozoic Deep-Sea Temperatures and Global Ice
575 Volumes from Mg/Ca in Benthic Foraminiferal Calcite. *Science*, 287(5451), pp.269–272.

576 Li, L. et al., 2011. A 4-Ma record of thermal evolution in the tropical western Pacific and its
577 implications on climate change. *Earth and Planetary Science Letters*, 309(1-2), pp.10–20.

578 Li, Y.-H., 1982. A brief discussion ont he mean oceanic residence time of elements. *Geochimica et*
579 *Cosmochimica Acta*, 46, pp.2671–2675.

580 Lisiecki, L.E. & Raymo, M.E., 2005. A Pliocene-Pleistocene stack of 57 globally distributed benthic
581 $\delta^{18}O$ records. *Paleoceanography*, 20(1).

582 Marchitto, T.M. et al., 2014. Improved oxygen isotope temperature calibrations for cosmopolitan
583 benthic foraminifera. *Geochimica et Cosmochimica Acta*, 130, pp.1–11.

584 Medina-Elizalde, M., Lea, D.W. & Fantle, M.S., 2008. Implications of seawater Mg/Ca variability for
585 Plio-Pleistocene tropical climate reconstruction. *Earth and Planetary Science Letters*, 269(3-4),
586 pp.585–595.

587 Miller, K.G. et al., 2012. High tide of the warm Pliocene: Implications of global sea level for Antarctic
588 deglaciation. *Geology*, 40(5), pp.407–410.

589 Mucci, A. & Morse, J.W., 1983. The incorporation of Mg *′ and Sr * + into calcite overgrowths:
590 influences of growth rate and solution composition. *Geochimica et Cosmochimica Acta*, 47,
591 pp.217–233.

592 Müller, W. et al., 2009. Initial performance metrics of a new custom-designed ArF excimer LA-
593 ICPMS system coupled to a two-volume laser-ablation cell. *Journal of Analytical Atomic*
594 *Spectrometry*, 24(2), p.209.

595 Nürnberg, D., Bijma, J. & Hemleben, C., 1996. Assessing the reliability of magnesium in
596 foraminiferal calcite as a proxy for water mass temperatures. *Geochimica et Cosmochimica*
597 *Acta*, 60(5), pp.803–814.

598 O'Brien, C.L. et al., 2014. High sea surface temperatures in tropicalwarm pools during the Pliocene.
599 *Nature Geoscience*, 7, pp.606-611.

600 Rausch, S. et al., 2013. Calcium carbonate veins in ocean crust record a threefold increase of
601 seawater Mg/Ca in the past 30 million years. *Earth and Planetary Science Letters*, 362, pp.215–
602 224.

603 Regenberg, M. et al., 2014. Global dissolution effects on planktonic foraminiferal Mg / Ca ratios
604 controlled by the calcite-saturation state of bottom waters. , pp.127–142.

605 Ries, J.B., 2004. Effect of ambient Mg/Ca ratio on Mg fractionation in calcareous marine
606 invertebrates: A record of the oceanic Mg/Ca ratio over the Phanerozoic. *Geology*, 32(11),
607 p.981.

608 Rosenthal, Y. & Lohmann, G.P., 2002. Accurate estimation of sea surface temperatures using
609 dissolution-corrected calibrations for Mg/Ca paleothermometry. *Paleoceanography*, 17(3),
610 pp.1–6.

611 Schmidt, M.W., Vautravers, M.J. & Spero, H.J., 2006. Western Caribbean sea surface temperatures
612 during the late Quaternary. *Geochemistry, Geophysics, Geosystems*, 7(2).

613 Segev, E. & Erez, J., 2006. Effect of Mg/Ca ratio in seawater on shell composition in shallow benthic
614 foraminifera. *Geochemistry Geophysics Geosystems*, 7(2), pp.1–8.

615 Seki, O. et al., 2010. Alkenone and boron-based Pliocene pCO2 records. *Earth and Planetary Science*
616 *Letters*, 292(1-2), pp.201–211.

617 Sosdian, S. & Rosenthal, Y., 2009. Deep-sea temperature and ice volume changes across the
618 Pliocene-Pleistocene climate transitions. *Science*, 325(5938), pp.306–10.

619 Sosdian, S. & Rosenthal, Y., 2010. Response to Comment on "Deep-Sea Temperature and Ice
620 Volume Changes Across the Pliocene-Pleistocene Climate Transitions." *Science*, 328(5985),
621 pp.1480–1480.

622 Tian, J. et al., 2006. Late Pliocene monsoon linkage in the tropical South China Sea. *Earth and*
623 *Planetary Science Letters*, 252(1-2), pp.72–81.

624 Wara, M.W., Ravelo, A.C. & Delaney, M.L., 2005. Permanent El Niño-like conditions during the
625 Pliocene warm period. *Science*, 309(5735), pp.758–61.

626 Woodard, S.C. et al., 2014. Antarctic role in Northern Hemisphere glaciation. *Science*, 346(6211)
627 pp.847-851.

628 Zachos, J.C. et al., 2003. A transient rise in tropical sea surface temperature during the Paleocene-
629 Eocene thermal maximum. *Science*, 302(5650), pp.1551–4.

630 Zhang, Y.G., Pagani, M. & Liu, Z., 2014. A 12-million-year temperature history of the tropical Pacific
631 Ocean. *Science*, 344(6179), pp.84–7.

632

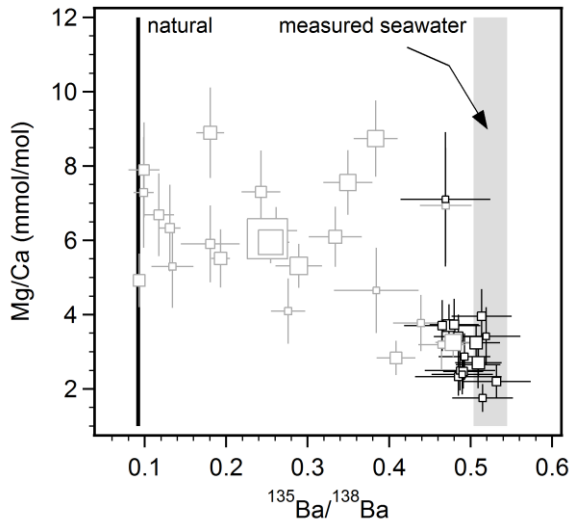

633

634 **Figure 1**. An example of the use of seawater isotopically-enriched with ^{135}Ba to unambiguously

635 identify material grown in culture. Experiment DE3-2-26 is shown as an example. Datapoints

636 represent mean values integrated from entire chamber wall profiles. This experiment was

637 characterised by Mg/Ca_{sw} = 2.2 mol mol^{-1} (~40% of modern), as a result chambers with elevated

638 $^{135}Ba/^{138}Ba$ have low Mg/Ca ratios. Analyses shown in black are those with $^{135}Ba/^{138}Ba$ within error of

639 the culture seawater, only these data were used to define the calibrations. Marker size is shown as a

640 function of analysis length, proportional to chamber wall thickness.

641

642 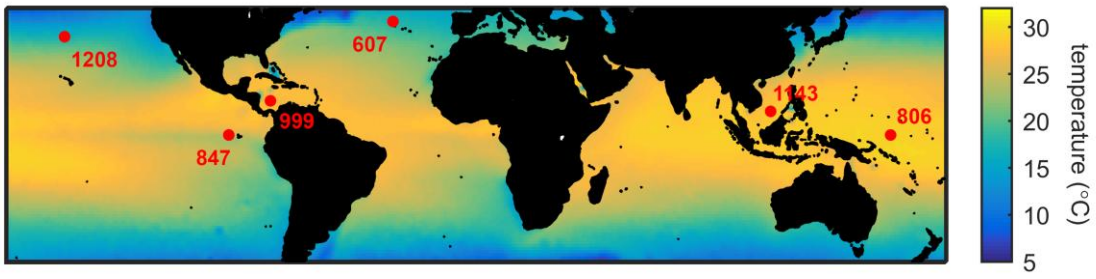

643 **Figure 2**. Map showing the location of the Deep Sea Drilling Program (607) and Ocean Drilling
644 Program sites from which published datasets were utilised for this study. Colour is shown as a
645 function of mean annual sea surface temperature.

646

647

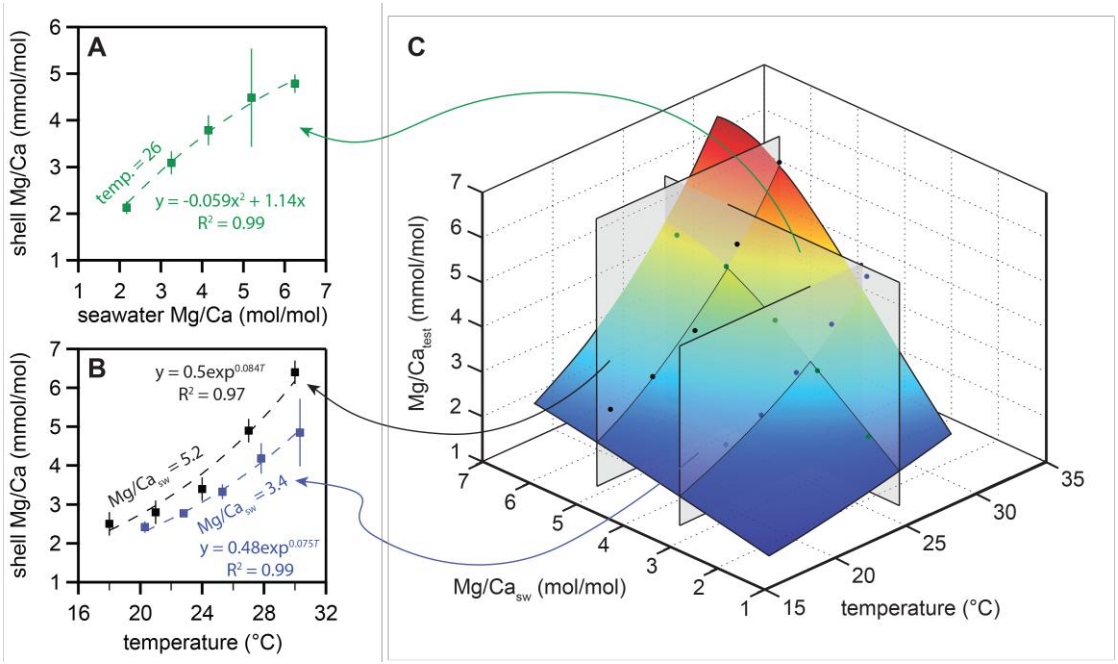

Figure 3. *G. ruber* laboratory calibrations. (A) Cultured relationship between Mg/Ca_{sw} and Mg/Ca_{test}, the relationship is nonlinear. (B) Mg/Ca_{test}-temperature calibration at Mg/Ca_{sw} = 3.4 mol mol^{-1}, in comparison to that in modern seawater (Mg/Ca_{sw} = 5.2 mol mol^{-1}) [Kisakürek et al. 2008]. (C) Coupled calibration surface based on least-squares modelling a surface to these three calibrations (see section 3.1 for model details). Using this surface, temperature or Mg/Ca_{sw} may be reconstructed if the other is constrained independently.

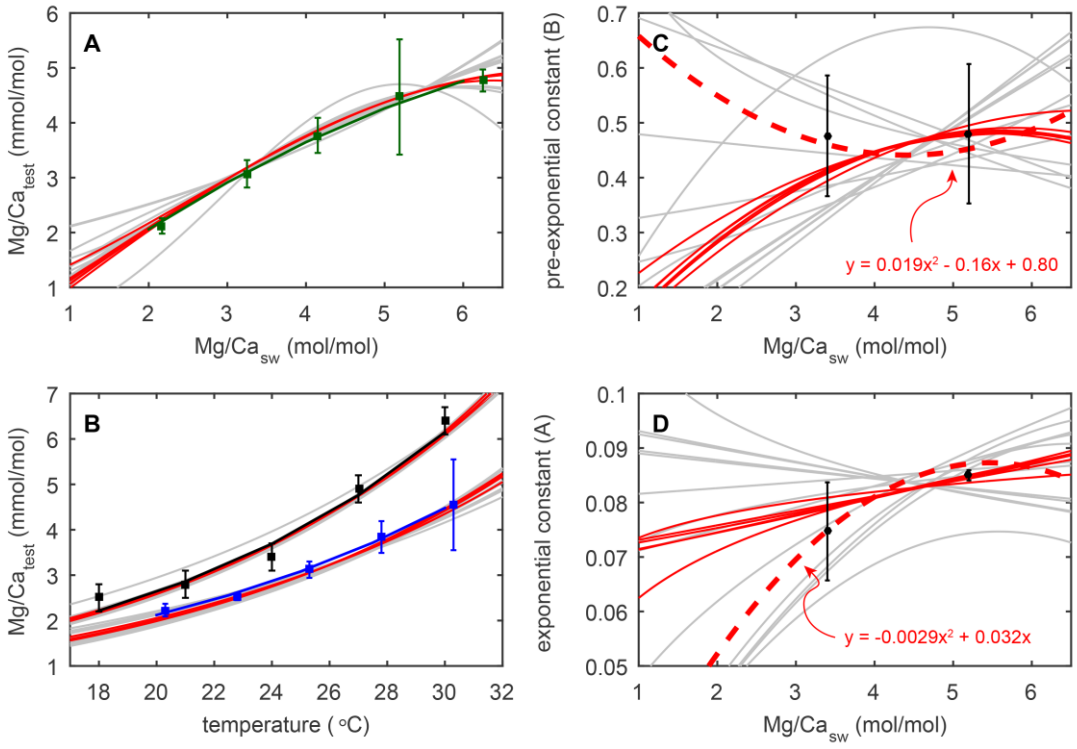

656

657 **Figure 4**. Least squares modelling the Mg/Ca_{sw}-Mg/Ca_{test}-temperature calibration lines in order to
658 produce an equation linking the three variables. Twenty different models were constructed based
659 on the assumption that Mg/Ca_{test} and temperature are always exponentially related, with different
660 assumptions regarding the way the two coefficients depend on Mg/Ca_{sw}. (A) and (B) show the
661 extent to which models constructed in this way accurately represent the empirical calibrations
662 (shown using the same colours as figure 3). (C) and (D) show the prediction that these models make
663 for the variation in the exponential and pre-exponential constants with changing Mg/Ca_{sw}. Red and
664 grey lines show models that deviated from the empirical calibrations by less and more than 0.1
665 mmol mol^{-1} on average respectively. The thick dashed red lines (both coefficients vary quadratically
666 with Mg/Ca_{sw}) show the model that best captures all aspects of Mg incorporation based on these
667 cultures.

668

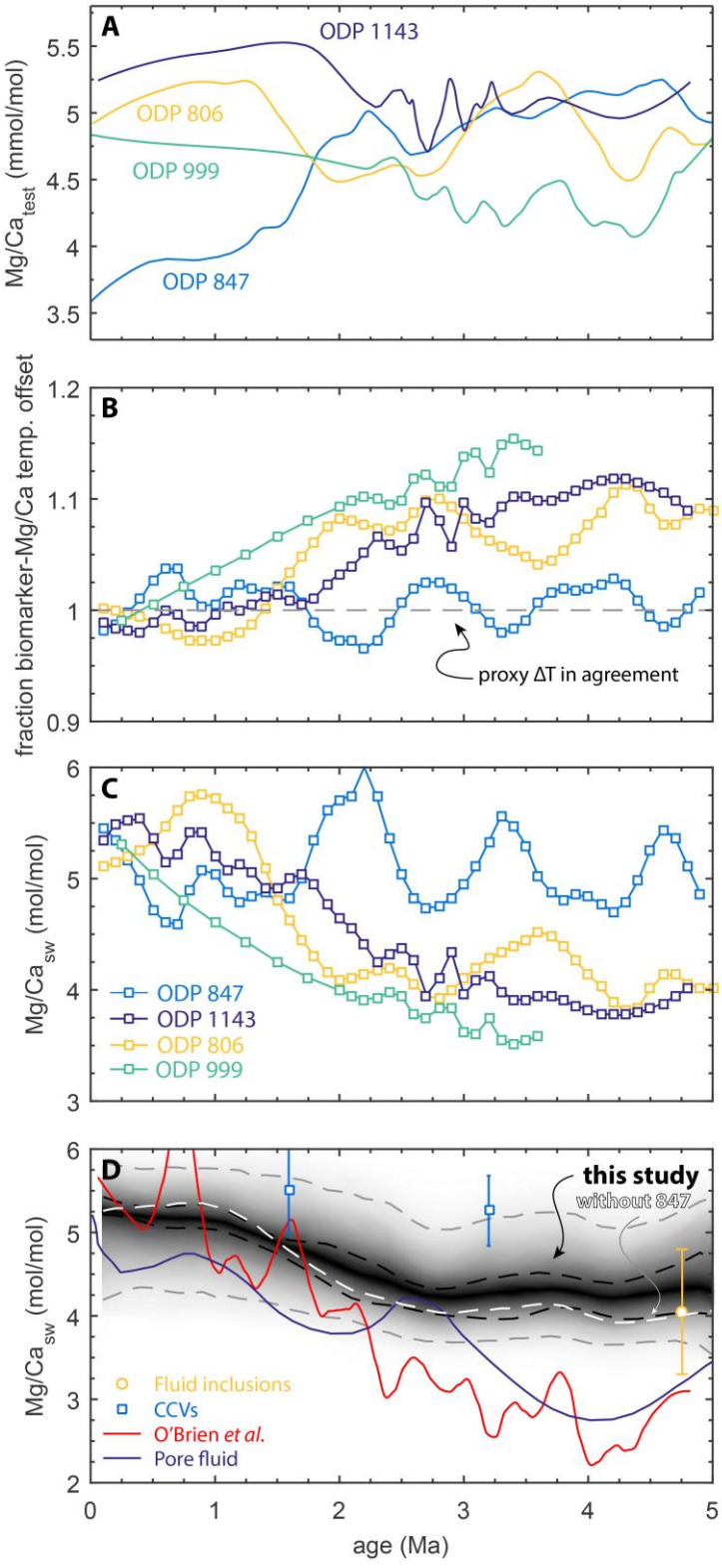

669

670 **Figure 5**. (A) Dissolution-corrected Mg/Ca records for the four tropical sites for which at least one

671 other palaeotemperature proxy is available for the last 5 Ma, see text for references. With the

672 exception of Site 847, all Mg/Ca records imply Pliocene SST lower than or the same as present day.

673 (B) Mg/Ca-biomarker proxy SST offset (Mg/Ca SST/biomarker SST). Pliocene TEX_{86} and alkenone-
674 derived SST are 5-15% higher compared to Mg/Ca, with the exception of Site 847. (C) Site-specific
675 back-calculated Mg/Ca_{sw} produced using the calibration surface shown in figure 3C, assuming that
676 the offsets in (B) are a result of secular Mg/Ca_{sw} variation. (D) Smoothed Mg/Ca_{sw} record produced
677 by combining data from all sites (shaded area, where shading is a function of probability), the thin
678 white line shows a similar curve produced without data from Site 847 (see text). Two sets of 95%
679 confidence bands are shown (black and grey dashed lines), estimated using a bootstrap approach,
680 see supporting material for details. The inner error bands account for intra-site variance in Mg/Ca_{sw}
681 reconstruction only, whilst the outer bands include a potential ±2.5°C offset between Mg/Ca and
682 the biomarker proxies compared to present day at any given site. Other proxy reconstructions (CCV
683 = ridge flank calcium carbonate veins) are shown for comparison [Fantle & DePaolo 2006; Rausch et
684 al. 2013; Horita et al. 2002], along with the Mg/Ca_{sw} record of O'Brien et al. [2014].
685

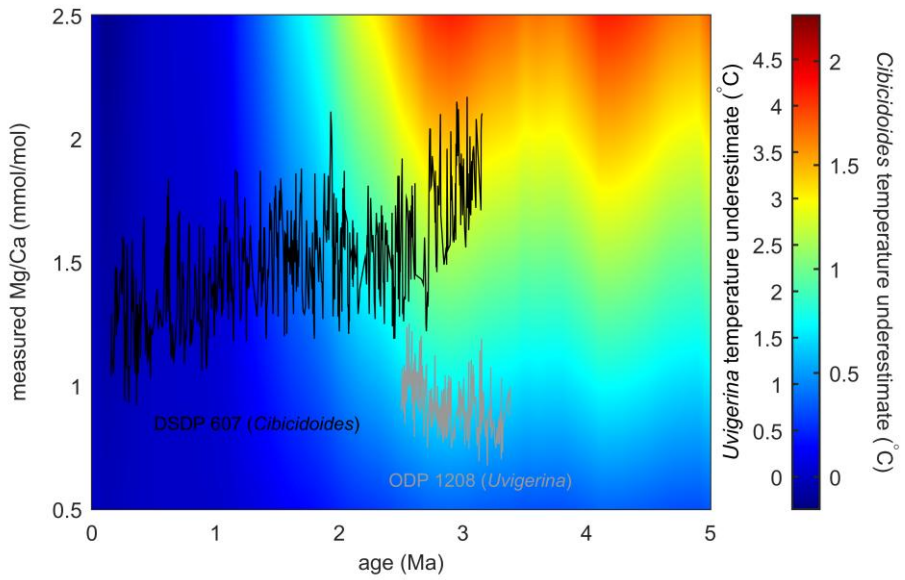

686

687 **Figure 6**. The error in foraminifera Mg/Ca-derived deep ocean temperature associated with
688 assuming no secular variation in Mg/Ca_{sw} over the last 5 Ma. Temperature underestimate is shown
689 as a function of colour, two published records are overlain [Sosdian & Rosenthal 2009; Woodard et
690 al. 2014]. The applicability of this graph to the species used to create these records (*Uvigerina* spp.,
691 *Cibicidoides wuellerstorfi* and *Oridorsalis umbonatus*) is based on the assumption that all of these
692 benthic foraminifera are characterised by identical Mg/Ca_{test}-Mg/Ca_{sw} relationships, and produced
693 using the Mg/Ca-temperature sensitivities of the studies from which the data are taken. For a given
694 measured Mg/Ca_{test} ratio, the *Uvigerina* temperature offset is much greater than that for
695 *Cibicidoides*. Benthic foraminifera Mg/Ca uncorrected for Mg/Ca_{sw} would result in a deep ocean
696 temperature underestimate of 0.9-1.4°C during the Pliocene.

697

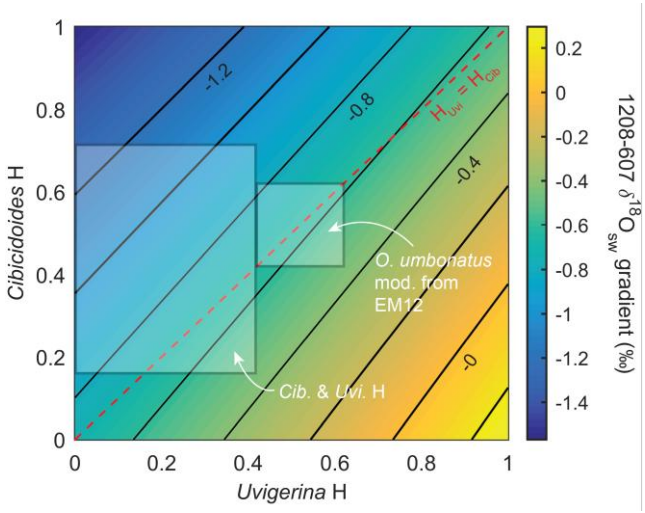

Figure 7. The effect of inter-species differences in H on the Site 1208-607 reconstructed Pliocene inter-basin $\delta^{18}O_{sw}$ gradient. Calculated values of H (the power component of a seawater-test Mg/Ca calibration) for *Cibicidoides* and *Uvigerina* from this study are shown in comparison to that for *O. umbonatus* [EM12; Evans & Müller 2012]. The previous estimate of this gradient [Woodard et al. 2014] of 0.7‰, derived assuming no seawater chemistry change, falls within the range we reconstruct ($\Delta\delta^{18}O_{sw}$ = -0.45 to -1.25), although we show that there is considerable uncertainty (±0.4‰) associated with this as H is likely different and loosely constrained for *Cibicidoides* and *Uvigerina*. Accurately characterising this relationship is a pre-requisite of reconstructing Pliocene inter-basin $\delta^{18}O_{sw}$ at sub-permil level accuracy if more than one species is used.

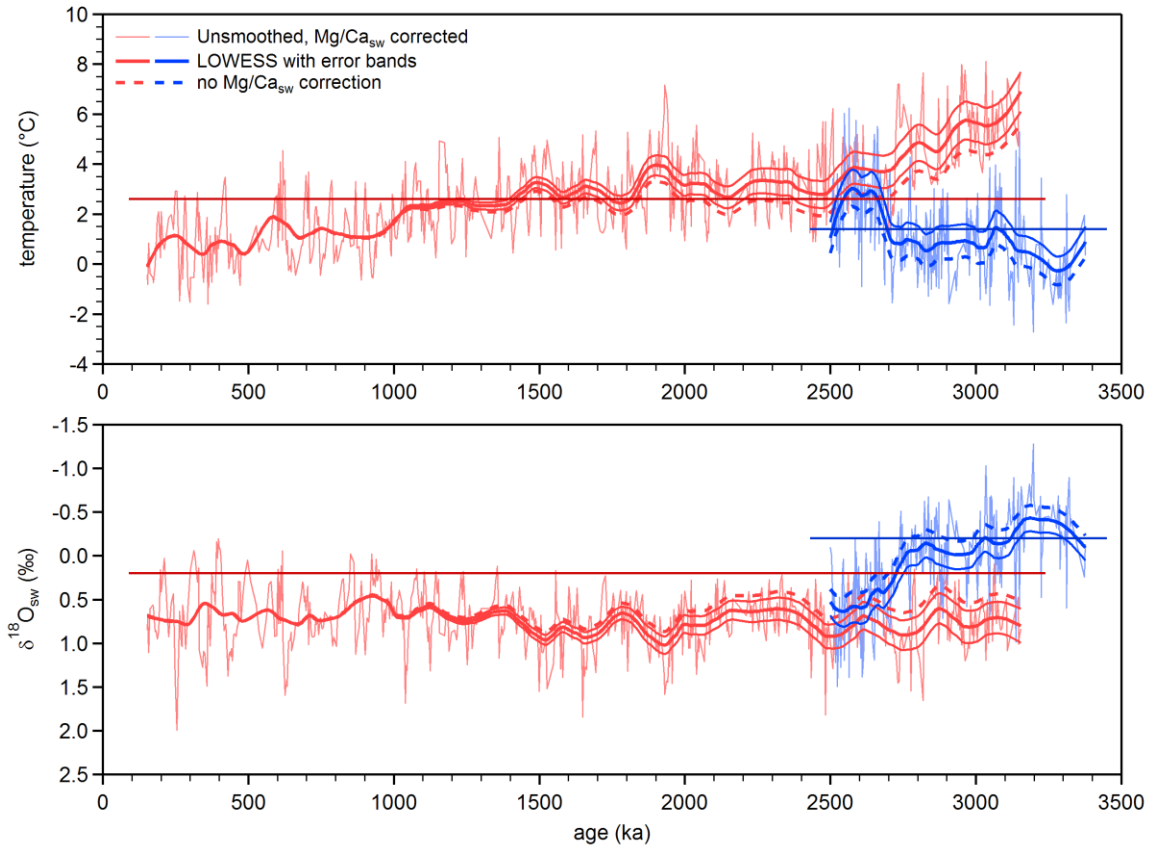

Figure 8. (A) The thermal evolution of the deep ocean at Site 607 (red lines) and Site 1208 (blue). Unsmoothed (thin) lines are shown without error bands, whilst smoothed (thick) lines are shown with bands representing the temporal variation in the magnitude of error in these reconstructions as a result of the uncertainty in H for each species. No uncertainty derived from the Mg/Ca-temperature calibration is shown, but is reported to be 0.8-1.1°C [Sosdian & Rosenthal 2009]. Dashed lines show the same record without correction for secular seawater chemistry variability. This dashed line forms one of the error limits for the Uvigerina-derived record from Site 1208 as this species has H within error of 0, with the implication that Mg incorporation into this foraminifera may be insensitive to Mg/Ca_{sw}, see text for details. The Mg/Ca-temperature calibrations used were those originally reported with the respective records. (B) $\delta^{18}O_{sw}$ reconstruction and uncertainty associated with the control exerted by Mg/Ca_{sw} on the Mg/Ca-derived temperatures used to calculate this from $\delta^{18}O_{test}$.

Table 1. Culture details. The number of analyses (n) that went into producing the mean foraminifera Mg/Ca values shown in the final three columns refers to the amount of chambers precipitated entirely in culture. $\Omega_{caclcite}$ (calcite saturation state) and $[CO_3^{2-}]$ were calculated from alkalinity and pH. Both measured and adjusted Mg/Ca (used for the coupled-calibration, see the supporting material) are shown.

	n	temp (°C)	Mg/Ca_{sw} (mol/mol)	alkalinity	$[CO_3^{2-}]$ (µM)	Ω	pH	$^{135}Ba/^{138}Ba$	2SE	Mg/Ca_{test} (mmol/mol)	Mg/Ca_{test} pH adj.	2SE
Variable Mg/Ca_{sw}; constant temperature												
DE3-6-26	12	26.3	6.25	2211.0	161.9	3.84	8.0	1.60	0.02	6.80	4.77	0.20
DE3-5-26	8	26.3	5.19	2263.6	165.9	3.93	8.0	1.83	0.02	6.37	4.47	1.05
DE3-4-26	22	26.3	4.15	2298.6	168.5	4.00	8.0	0.98	0.04	5.38	3.77	0.32
DE3-3-26	15	26.3	3.25	2352.3	172.6	4.09	8.0	0.63	0.07	4.38	3.07	0.25
DE3-2-26	19	26.3	2.17	2477.0	182.1	4.32	8.0	0.52	0.06	3.03	2.12	0.14
Variable temperature; constant Mg/Ca_{sw}												
DE4-3-30	2	30.3	3.40	2532.4	286.1	6.83	8.2	1.72	0.07	4.55	-	1.00
DE4-3-27.5	4	27.8	3.40	2532.4	271.1	6.44	8.2	1.72	0.07	3.84	-	0.35
DE4-3-25	27	25.3	3.40	2412.7	243.5	5.77	8.2	1.71	0.07	3.12	-	0.18
DE4-3-22.5	6	22.8	3.40	2412.7	229.7	5.42	8.2	1.71	0.06	2.53	-	0.08
DE4-3-20	5	20.3	3.40	2412.7	216.0	5.09	8.2	1.71	0.06	2.23	-	0.14